

Transverse mass and invariant mass observables for measuring the mass of a semi-invisibly decaying heavy particle.

Daniel R. Tovey,

*Department of Physics and Astronomy,
University of Sheffield, Hounsfield Road, Sheffield S3 7RH, UK
E-mail: daniel.tovey@cern.ch*

ABSTRACT: Formulae are derived for the positions of end-points in the invariant mass and transverse mass distributions obtained from the products of heavy states decaying to pairs of semi-invisibly decaying lighter states. Formulae are derived both for the special case where the two decay chains are identical and the more general case where they are different. The formulae are tested with a simple case study of heavy SUSY higgs particles decaying to gauginos at the LHC.

KEYWORDS: SUSY, Higgs.

Contents

1. Introduction	1
2. Invariant mass end-points	2
2.1 Identical chains	3
2.2 Non-identical chains	4
3. Transverse mass end-points	7
3.1 Identical chains	8
3.2 Non-identical chains	9
4. Example: SUSY higgs decaying to gauginos at the LHC	9
5. Conclusions	11

1. Introduction

In recent years there has been considerable theoretical and experimental interest in the possibility of observing and measuring the production of heavy neutral SUSY higgs particles (H/A) at the LHC. In many regions of parameter space decays to Standard Model (SM) particles such as $H/A \rightarrow \tau\tau$ provide the clean signature of a peak at $m(H/A)$ in the reconstructed invariant mass distribution of the decay products. In certain regions of parameter space however, particularly at larger values of m_A , this channel is suppressed and alternative signatures must be sought. One interesting possibility [1, 2, 3, 4, 5, 6, 7, 8, 9, 10, 11, 12, 13] involves the use of higgs decays to pairs of gauginos (neutralinos or charginos), with subsequent gaugino decays to dileptons and the Lightest Supersymmetric Particle (LSP – here assumed to be neutral and stable). The resulting $4\ell + E_T^{\text{miss}}$ signature suffers from relatively little irreducible Standard Model background contamination, although there can be significant irreducible SUSY background from direct or indirect gaugino production (the latter via squark decays).

Several detailed studies have been performed of the likely sensitivity of the LHC detectors to SUSY higgs production using the $4\ell + E_T^{\text{miss}}$ signature (see e.g. Refs. [1, 2, 3, 4, 5, 6, 7, 8, 9, 10, 11, 12, 13]). If a statistically significant excess is observed in this channel then it is natural to ask whether the same channel can be used to measure the mass of the higgs. Unlike in the case of SM decays it is likely to be extremely difficult to reconstruct a higgs mass peak due to the presence of the two heavy invisible LSPs in each higgs decay. In the case where the decay proceeds through the chain:

$$H/A \rightarrow \tilde{\chi}_2^0 \tilde{\chi}_2^0 \rightarrow \ell\tilde{\ell}\ell\tilde{\ell} \rightarrow \ell\ell\ell\ell\tilde{\chi}_1^0\tilde{\chi}_1^0, \quad (1.1)$$

and the masses of the $\tilde{\chi}_2^0$, $\tilde{\ell}$ and $\tilde{\chi}_1^0$ (LSP) are known, it is possible to solve the kinematic constraints to obtain an event-by-event value of $m(H/A)$ [6]. If the sleptons $\tilde{\ell}$ are heavy however, causing the $\tilde{\chi}_2^0$ particles decay through the three-body process $\tilde{\chi}_2^0 \rightarrow \ell\ell\tilde{\chi}_1^0$, there are insufficient constraints to solve for $m(H/A)$. In this case one must resort to measuring the positions of end-points in the distributions of event invariant mass and transverse mass [14, 15, 16, 17, 18, 19, 20] values, which depend on the masses of all the particles involved in the decay, including $m(H/A)$.

In this brief paper we shall derive formulae for the positions of these end-points both in the special case where the decay chains are identical and in the more general case of non-identical decay chains. The resulting expressions will be applicable to any channel in which a heavy state ω decays to a pair of lighter states δ_i ($i = 1, 2$), each of which decays in turn to an aggregate visible state v_i and an invisible particle α_i :

$$\omega \rightarrow \delta_1 \delta_2 \rightarrow v_1 \alpha_1 v_2 \alpha_2. \quad (1.2)$$

Note that the aggregate visible states v_i can each be composed of multiple visible particles – the v_i should be considered to be pseudo-particles with four-momenta equal to the net four-momenta of their constituents. We shall test the new formulae with a simple case-study of heavy SUSY higgs decays to gauginos. We shall not attempt to perform a full detector-level study of the SM and SUSY backgrounds to the $4\ell + E_T^{\text{miss}}$ channel as this is described elsewhere (see e.g. Refs. [4, 9, 12, 13]), however we shall discuss the relative merits of using the invariant mass and transverse mass end-points to measure $m(H/A)$.

The structure of the paper is as follows. In Section 2 we derive the invariant mass end-point formulae while in Section 3 we derive the equivalent formulae for transverse mass end-points. In Section 4 we present the results of the case-study of SUSY higgs decays to four leptons and E_T^{miss} . In Section 5 we conclude.

2. Invariant mass end-points

As is well-known the invariant mass of the aggregate visible products of each chain, v_1 and v_2 , is given by:

$$\begin{aligned} m^2(v_1, v_2) &= [E(v_1) + E(v_2)]^2 - [\mathbf{p}(v_1) + \mathbf{p}(v_2)]^2 \\ &= m^2(v_1) + m^2(v_2) + 2[E(v_1)E(v_2) - \mathbf{p}(v_1) \cdot \mathbf{p}(v_2)], \end{aligned} \quad (2.1)$$

where bold quantities denote three-momenta. The maximum value taken by $m(v_1, v_2)$ depends upon whether the α_i particles can be brought to rest in the ω rest frame. Such a configuration can be obtained in principle if the boosts of the α_i particles in the respective δ_i rest frames can be arranged to exactly cancel the boosts they obtain in the ω rest frame from the boosts of the δ_i rest frames. If this condition can be satisfied for some values of $m(v_i)$ then this configuration generates the maximum possible value of $m(v_1, v_2)$:

$$m_{\text{max}}(v_1, v_2) = m(\omega) - m(\alpha_1) - m(\alpha_2). \quad (2.2)$$

The necessary and sufficient conditions imposed upon the masses by this condition are discussed below for the cases where the two δ_i decay chains are identical or different.

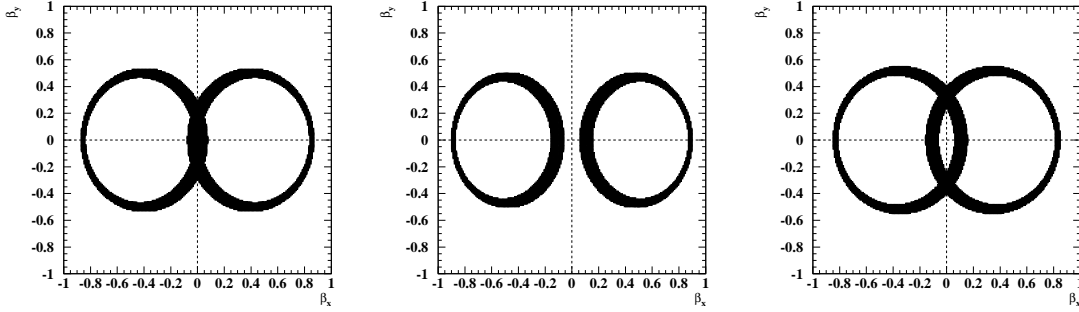


Figure 1: α_i phase space diagrams for toy models with identical decay chains. The hatched regions represent the annular rings referred to in the text. See text for details of models.

2.1 Identical chains

When δ_1 and δ_2 are of equal mass, and similarly for α_1 and α_2 , the condition that both α_i particles be brought to rest in the ω rest frame is equivalent to the requirement:

$$m_{\max}^2(v) \geq m^2(\delta) - m(\alpha)[m(\omega) - m(\alpha)] \geq m_{\min}^2(v), \quad (2.3)$$

where $m_{\max}(v)$ and $m_{\min}(v)$ are respectively the maximum and minimum possible invariant masses of all the visible decay products of each chain. If this condition can be satisfied then from Eqn. (2.2)

$$m_{\max}(v_1, v_2) = m(\omega) - 2m(\alpha). \quad (2.4)$$

In models satisfying Eqn. (2.3) the kinematic configuration saturating the bound Eqn. (2.4) is that in which both α_i particles are emitted against the motion of their parent δ_i particles with sufficient momentum to cancel the boost in the ω rest frame provided by this motion.

A useful means of visualising the kinematic configurations generated by a given model is provided by phase-space diagrams in which the cylindrical polar components of the velocities β of the two α_i particles measured in the ω rest frame are plotted on the \hat{x} axis (components parallel to the ω decay axis) and \hat{y} axis (components perpendicular to the ω decay axis). Examples of such diagrams are shown in Figure 1. In these diagrams the phase space accessible to each α_i particle is represented by an annular ring, with the outer and inner boundaries defined by the kinematic configurations in which $m(v_i) = m_{\min}(v_i)$ and $m(v_i) = m_{\max}(v)$ respectively. If $m_{\max}(v) = m(\delta_i) - m(\alpha_i)$, as is the case for three-body δ_i decays, then the inner boundary possesses zero radius. This is because in this case the α_i particles must be produced at rest in the δ_i rest frames.

Figure 1(left) shows the α_i phase space diagram for a toy model satisfying Eqn. (2.3). The configuration saturating the bound Eqn. (2.3) is that in which $\beta = 0$ for both α_i particles, which requires that the origin lies within both annular regions.

Figure 1(centre) and Figure 1(right) show α_i phase space diagrams for models which do not satisfy Eqn. (2.3), as can easily be seen by observing that in neither case does the origin lie within the annular regions. In such cases $m_{\max}(v_1, v_2)$ is obtained from configurations

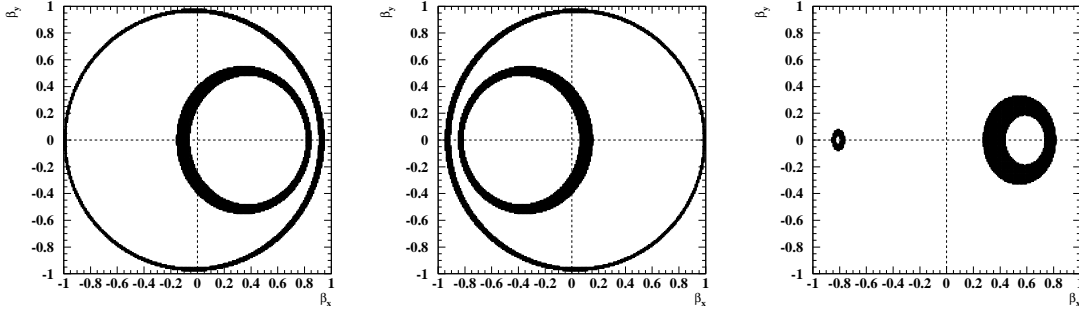


Figure 2: α_i phase space diagrams for toy models with non-identical decay chains. The left(right)-hand annular regions in each figure correspond to decay chain 1(2). See text for details of models.

in which $m(\alpha_1, \alpha_2)$ is minimised. These configurations must therefore simultaneously minimise the velocity β of each α_i particle in the ω rest frame. In models similar to that shown in Figure 1(centre) this requires that $m(v_1) = m(v_2) = m_{\min}(v)$, generating configurations lying on the outer boundaries of the annular regions. In Figure 1(right) this requires that $m(v_1) = m(v_2) = m_{\max}(v)$ generating configurations lying on the inner boundaries. In both cases the configurations saturating the bound generate β values lying on the \hat{x} -axis. This can be understood by remembering that the closest point to the origin on a circle with centre displaced from the origin along a given axis lies at the intersection between that axis and the circle.

In practice, if Eqn. (2.3) is not satisfied for a given model then $m_{\max}(v_1, v_2)$ can be determined from the maximum of the two values of $m(v_1, v_2)$ obtained when $m(v_1) = m(v_2) = m_{\max}(v)$ and $m(v_1) = m(v_2) = m_{\min}(v)$, assuming that both α_i particles are emitted against the directions of motion of their parent δ_i particles. For fixed $m(v_1) = m(v_2) = m(v)$ this configuration leads to the following expression for $m(v_1, v_2)$:

$$m(v_1, v_2) = \frac{m(\omega)}{2m^2(\delta)} \left[m^2(\delta) - m^2(\alpha) + m^2(v) + \frac{1}{m(\omega)} \sqrt{(m^2(\omega) - 4m^2(\delta)) ([m^2(\delta) - m^2(\alpha) + m^2(v)]^2 - 4m^2(\delta)m^2(v))} \right], \quad (2.5)$$

and so substituting respectively $m(v) = m_{\max}(v)$ and $m(v) = m_{\min}(v)$ into Eqn. (2.5) enables $m_{\max}(v_1, v_2)$ to be determined.

2.2 Non-identical chains

When the two decay chains are not identical alternative kinematic configurations can maximise $m(v_1, v_2)$. In such models the α_i phase space diagrams are not in general symmetric and qualitatively new configurations can be generated such as those appearing in the diagrams in Figure 2. In Figure 2(left) and Figure 2(centre) the energy released in the decay of δ_1 is respectively less than or greater than that released in the decay of δ_2 . In Figure 2(right) $m(\delta_2)$ is very much less than $m(\delta_1)$ leading to a larger boost of δ_2 and hence a larger offset of the centre of the left-hand annular region. It should be clear from

this diagram that the number of kinematic configurations which can in principle maximise $m(v_1, v_2)$ is greater than in the case of identical decay chains.

As in the case of identical decay chains discussed above, the maximum possible value of $m(v_1, v_2)$ is given by Eqn. (2.2) if the model can generate a configuration in which both α_i particles are at rest in the ω rest frame. The conditions for this to be the case for non-identical decay chains, analogous to Eqn. (2.3) for identical decay chains are:

$$m_{\max}^2(v_1) \geq m^2(\delta_1) - m(\alpha_1) \left[m(\omega) - m(\alpha_1) + \frac{m^2(\delta_1) - m^2(\delta_2)}{m(\omega)} \right] \geq m_{\min}^2(v_1), \quad (2.6)$$

$$m_{\max}^2(v_2) \geq m^2(\delta_2) - m(\alpha_2) \left[m(\omega) - m(\alpha_2) + \frac{m^2(\delta_2) - m^2(\delta_1)}{m(\omega)} \right] \geq m_{\min}^2(v_2). \quad (2.7)$$

To identify the possible configurations which can maximise $m(v_1, v_2)$ when the conditions Eqns. (2.6) and (2.7) are not satisfied let us first consider the energies and momenta of the α_i and v_i particles in the δ_i rest frames. These may be determined from simple two-body kinematics to be:

$$\begin{aligned} E(\alpha_1) &= \frac{m^2(\delta_1) + m^2(\alpha_1) - m^2(v_1)}{2m(\delta_1)}, & E(v_1) &= \frac{m^2(\delta_1) - m^2(\alpha_1) + m^2(v_1)}{2m(\delta_1)}, \\ E(\alpha_2) &= \frac{m^2(\delta_2) + m^2(\alpha_2) - m^2(v_2)}{2m(\delta_2)}, & E(v_2) &= \frac{m^2(\delta_2) - m^2(\alpha_2) + m^2(v_2)}{2m(\delta_2)}, \end{aligned} \quad (2.8)$$

and

$$\begin{aligned} p(v_1) &= p(\alpha_1) = \sqrt{E^2(v_1) - m^2(v_1)} = \sqrt{E^2(\alpha_1) - m^2(\alpha_1)}, \\ p(v_2) &= p(\alpha_2) = \sqrt{E^2(v_2) - m^2(v_2)} = \sqrt{E^2(\alpha_2) - m^2(\alpha_2)}, \end{aligned} \quad (2.9)$$

where $p(x)$ denotes the magnitude of the three-momentum of particle x . In addition the energies and momenta of the δ_i particles in the ω rest frame are given by:

$$E(\delta_1) = \frac{m^2(\omega) + m^2(\delta_1) - m^2(\delta_2)}{2m(\omega)}, \quad E(\delta_2) = \frac{m^2(\omega) - m^2(\delta_1) + m^2(\delta_2)}{2m(\omega)}, \quad (2.10)$$

and

$$p(\delta_1) = p(\delta_2) = \sqrt{E^2(\delta_1) - m^2(\delta_1)} = \sqrt{E^2(\delta_2) - m^2(\delta_2)}. \quad (2.11)$$

The magnitudes of the boosts β_i provided to the δ_i particles by the ω decay can be obtained from

$$\beta_i = \frac{p(\delta_i)}{E(\delta_i)}. \quad (2.12)$$

Now let us consider the possible extremal values of the momenta and energies of the α_i and v_i particles in the ω rest frame, for fixed $m(v_1)$ and $m(v_2)$. These can be obtained through Lorentz transformations of Eqns. (2.8) and (2.9) with β_i values obtained from Eqns. (2.10)–(2.12):

$$\begin{aligned} E'(\alpha_1) &= \gamma_1[E(\alpha_1) + c_1\beta_1p(\alpha_1)], & p'(\alpha_1) &= \gamma_1[c_1p(\alpha_1) + \beta_1E(\alpha_1)], \\ E'(\alpha_2) &= \gamma_2[E(\alpha_2) - c_2\beta_2p(\alpha_2)], & p'(\alpha_2) &= \gamma_2[c_2p(\alpha_2) - \beta_2E(\alpha_2)], \\ E'(v_1) &= \gamma_1[E(v_1) - c_1\beta_1p(v_1)], & p'(v_1) &= \gamma_1[-c_1p(v_1) + \beta_1E(v_1)], \end{aligned}$$

$$E'(v_2) = \gamma_2[E(v_2) + c_2\beta_2 p(v_2)], \quad p'(v_2) = \gamma_2[-c_2 p(v_2) - \beta_2 E(v_2)], \quad (2.13)$$

where primed quantities are measured in the ω rest frame and γ_i is the Lorentz gamma factor derived from β_i . The quantities $c_i = \pm 1$ and are determined by the directions in which the α_i particles are emitted in the δ_i rest frames. If we define δ_1 to be travelling in the $+\hat{x}$ direction in the ω rest frame then $c_1 = +1$ corresponds to a configuration in which α_1 is emitted co-linearly with δ_1 , while if $c_1 = -1$ it is emitted contra-linearly. If $c_2 = +1$ then α_2 is emitted contra-linearly with δ_2 , while if $c_2 = -1$ it is emitted co-linearly. The α_i particles in these extremal configurations possess velocities given by $p'(\alpha_i)/E'(\alpha_i)$. When $m(v_1)$ or $m(v_2)$ are maximised or minimised these velocities define the coordinates at which the boundaries of the annular regions in α_i phase space diagrams such as Figure 1 cross the \hat{x} axes. The invariant masses of the visible particles in these extremal configurations can be obtained by substituting the energies and momenta of v_1 and v_2 from Eqns. (2.13) into Eqn. (2.1).

Now let us consider the kinematic configurations which generate extremal values of $m(v_1, v_2)$. We shall label these configurations with the signs of the c_i quantities, which denote the directions of the α_i particles in the δ_i rest frames, together with the masses of the v_i particles. The notation we shall use is of the form $\{\pm_v, \pm_w\}$, where the first(second) element inside the brackets refers to particle 1(2), the signs correspond to the signs of c_i , and the subscripts v and w describe the values of respectively $m(v_1)$ and $m(v_2)$. So for example $\{+_{\max}, -_{\min}\}$ corresponds to a configuration in which α_1 is emitted co-linearly with δ_1 , α_2 is emitted co-linearly with δ_2 , $m(v_1) = m_{\max}(v_1)$ and $m(v_2) = m_{\min}(v_2)$.

Using our new notation, the possible configurations maximising $m(v_1, v_2)$ in the case of identical decay chains discussed in Section 2.1 are $\{-_{\min}, +_{\min}\}$, corresponding to Figure 1(centre), and $\{-_{\max}, +_{\max}\}$, corresponding to Figure 1(right). In the case of non-identical decay chains we must also consider $\{-_{\max}, +_{\min}\}$ and $\{-_{\min}, +_{\max}\}$. We have not exhausted the possibilities however. In order to maximise $m(v_1, v_2)$ we must minimise both $m(\alpha_1, \alpha_2)$ and the net momentum of the $\alpha_1\alpha_2$ system. In some models with highly asymmetric decay chains, for example that represented in Figure 2(right), these two requirements are mutually exclusive – decreasing $m(\alpha_1, \alpha_2)$ increases the net invisible momentum and vice versa. In such models we must find the values of $m(v_1)$ and $m(v_2)$ which maximise $m(v_1, v_2)$ when respectively $m(v_2)$ and $m(v_1)$ are maximised or minimised. These values are located at the turning points of $m(v_1, v_2)$ and are given by:

$$m_{\text{tp}}^2(v_i) = m^2(\delta_i) + m^2(\alpha_i) - m(\alpha_i) \frac{2m^2(\delta_i)m(\delta_j) + AE(v_j) + Bp(v_j)}{\sqrt{m^2(\delta_j)[m^2(\delta_i) + m^2(v_j)] + m(\delta_j)[AE(v_j) + Bp(v_j)]}}, \quad (2.14)$$

where

$$A \equiv m^2(\omega) - m^2(\delta_1) - m^2(\delta_2), \quad B \equiv \sqrt{A^2 - 4m^2(\delta_1)m^2(\delta_2)}, \quad (2.15)$$

$E(v_j)$ and $p(v_j)$ are defined by Eqns. (2.8) and (2.9), and $j \neq i$. Taking all possible combinations into account this leads finally to eight possible values for $m_{\max}(v_1, v_2)$ when

Eqns. (2.6) and (2.7) are not satisfied. These values are obtained from the configurations:

$$\begin{aligned} &\{-\min, +\min\}, \{-\max, +\max\}, \{-\min, +\max\}, \{-\max, +\min\}, \\ &\{-\text{tp}, +\min\}, \{-\text{tp}, +\max\}, \{-\min, +\text{tp}\}, \{-\max, +\text{tp}\}. \end{aligned} \quad (2.16)$$

The value of $m_{\max}(v_1, v_2)$ is given by the maximum value of Eqn. (2.1) obtained by substituting the energies and momenta from Eqns. (2.13) for the eight configurations listed in Eqn. (2.16).

3. Transverse mass end-points

The transverse mass M_T of a set of visible and invisible decay products can be calculated from their transverse momenta and masses. The transverse momentum and mass of the aggregate visible decay product V of ω can be obtained by summing the four-momenta of the aggregate visible decay products v_1 and v_2 of each decay chain, while the transverse momentum of the invisible decay products is measured by the event E_T^{miss} vector. The optimum definition of M_T depends upon the value of the lower limit χ on the mass of the aggregate invisible decay product¹. If this limit is zero, for instance because the $m(\alpha_i)$ are unknown, then the optimum definition is:

$$M_T^2(0) \equiv m^2(V) + 2[E_T(V)E_T^{\text{miss}} - p_x(V)p_x^{\text{miss}} - p_y(V)p_y^{\text{miss}}], \quad (3.1)$$

where

$$E_T(V) \equiv \sqrt{p_T^2(V) + m^2(V)}. \quad (3.2)$$

A configuration which maximises $M_T(0)$ is that in which $m(V)$ is minimised and $p_T(V)$ is maximised. This requirement implies that δ_1 , δ_2 , α_1 , α_2 , v_1 and v_2 must all move in the laboratory transverse plane.

If the lower limit on the mass of the aggregate invisible decay product is non-zero, for instance because the $m(\alpha_i)$ have been measured, then the optimum definition is:

$$M_T^2(\chi) \equiv m^2(V) + \chi^2 + 2[E_T(V)E_T^{\text{miss}}(\chi) - p_x(V)p_x^{\text{miss}} - p_y(V)p_y^{\text{miss}}], \quad (3.3)$$

where

$$E_T^{\text{miss}}(\chi) \equiv \sqrt{(E_T^{\text{miss}})^2 + \chi^2}. \quad (3.4)$$

If the $m(\alpha_i)$ are known then a conservative value for χ is $m(\alpha_1) + m(\alpha_2)$, which we shall use below. The absolute maximum value of $M_T(m(\alpha_1) + m(\alpha_2))$ is $m(\omega)$, which is obtained when the α_1 is at rest with respect to α_2 , and δ_1 , δ_2 , α_1 , α_2 , v_1 and v_2 are all moving in the laboratory transverse plane. Given the discussion of Section 2, we can use α_i phase space diagrams such as Figures 1 and 2 to identify the configurations which satisfy this requirement. Note however that because we are now using only transverse momenta we must reinterpret such diagrams as representing the transverse cartesian components of velocity rather than cylindrical polar components about the ω decay axis. It is then clear

¹Note that this is not directly a limit on the mass of the individual invisible decay products α_i , for instance the LSPs in SUSY models.

that the configurations for which $M_T(m(\alpha_1) + m(\alpha_2)) = m(\omega)$ are those located in the regions of the α_i phase space diagram in which the annular regions overlap, provided all the motion lies in the laboratory transverse plane. If the annular regions for a given model do not overlap, or some of the particles move out of the laboratory transverse plane, then this bound is not saturated.

3.1 Identical chains

In the case of identical decay chains $M_T(0)$ defined by Eqn. (3.1) can be maximised with the configurations $\{+_{\min}, +_{\min}\}$ and $\{-_{\min}, -_{\min}\}$, which generate in this case equal maxima. Substituting Eqns. (2.13) into Eqn. (3.1) and assuming that all the motion lies in the laboratory transverse plane we obtain the bound:

$$M_T^{\max}(0) = \frac{m(\omega)}{2m^2(\delta)} \left[m^2(\delta) - m^2(\alpha) + m_{\min}^2(v) + \sqrt{[m^2(\delta) - m^2(\alpha) + m_{\min}^2(v)]^2 - 4m^2(\delta)m_{\min}^2(v)} \right], \quad (3.5)$$

where $m_{\min}(v)$ is the minimum value of the invariant mass of the *individual* aggregate visible decay products v_1 and v_2 , as in Section 2. If $m_{\min}(v) = 0$ this reduces to

$$M_T^{\max}(0) = m(\omega) \left[1 - \frac{m^2(\alpha)}{m^2(\delta)} \right], \quad (3.6)$$

which is always less than $m(\omega)$.

In the case of $M_T(m(\alpha_1) + m(\alpha_2))$, i.e. $M_T(2m(\alpha))$, the condition that $M_T^{\max}(2m(\alpha)) = m(\omega)$ is equivalent to requiring

$$m^2(\delta) - m(\alpha)[m(\omega) - m(\alpha)] \geq m_{\min}^2(v), \quad (3.7)$$

which is a less stringent requirement than Eqn. (2.3). Models satisfying this requirement include those represented in both Figure 1(left) and Figure 1(right). In the latter case the configurations saturating the bound possess α_i particles moving with $\beta_x = 0$ and $\beta_y \neq 0$, in other words emitted transverse to the δ_i direction in the ω rest frame. The fact that for a given model multiple configurations can saturate the bound rather than just one (as is the case for $m(v_1, v_2)$) shows that in principle the $M_T(2m(\alpha))$ end-point can be more prominent, as shall be discussed in Section 4.

If the requirement Eqn. (3.7) is not satisfied, as is the case for the model represented in Figure 1(centre), then the configuration which maximises $M_T(2m(\alpha))$ is that which minimises $m(\alpha_1, \alpha_2)$, with all the motion in the laboratory transverse plane. This configuration is $\{-_{\min}, +_{\min}\}$, which is also that configuration which maximises $m(v_1, v_2)$ given $m(v) = m_{\min}(v)$ (see Section 2.1). In this case the aggregate invisible and visible transverse momenta are zero and thus from Eqn. (3.3):

$$M_T^{\max}(2m(\alpha)) = 2m(\alpha) + m(v_1, v_2), \quad (3.8)$$

or equivalently from Eqn. (2.5):

$$M_T^{\max}(2m(\alpha)) = 2m(\alpha) + \frac{m(\omega)}{2m^2(\delta)} \left[m^2(\delta) - m^2(\alpha) + m_{\min}^2(v) + \frac{1}{m(\omega)} \sqrt{(m^2(\omega) - 4m^2(\delta))([m^2(\delta) - m^2(\alpha) + m_{\min}^2(v)]^2 - 4m^2(\delta)m_{\min}^2(v))} \right]. \quad (3.9)$$

3.2 Non-identical chains

In the case of non-identical decay chains the analysis for $M_T(0)$ is very similar to that in the case of identical decay chains. Configurations which can generate the maximum values of $M_T(0)$ are again $\{+\min, +\min\}$ and $\{-\min, -\min\}$, although in this case they may in principle generate different values of $M_T^{\max}(0)$. Assuming that all the motion lies in the laboratory transverse plane, these configurations can be used with Eqns. (2.13) and (3.1) to generate two possible values of $M_T^{\max}(0)$ with the maximum of these two values used.

When considering $M_T(m(\alpha_1) + m(\alpha_2))$ the analysis is more complicated. To simplify the discussion we shall first define decay chain 1 to be that chain which generates the smaller annular region in the α_i phase space diagram (see e.g. Figure 2). In other words we label decay chains such that the difference in β values for α_1 configurations $+\min$ and $-\min$ is less than the difference in β values for α_2 configurations $+\min$ and $-\min$. Given that we have already defined the $+\hat{x}$ direction to be that direction in which δ_1 is emitted in the ω rest frame, this additional definition then maps Figure 2(centre) onto Figure 2(left).

With this new definition of decay chains 1 and 2 we find that the requirement that the two annular regions in the α_i phase space diagram overlap is equivalent to requiring that the β value for the α_1 configuration $-\min$ is less than the β value for the α_2 configuration $+\min$, and the β value for the α_1 configuration $+\min$ is greater than the β value for the α_2 configuration $+\max$. These requirements are not satisfied by any of the three models represented in Figure 2 and in such cases the maximum value of $M_T(m(\alpha_1) + m(\alpha_2))$ is obtained from one of three configurations: $\{-\min, +\min\}$ (as in the case of identical chains), $\{-\max, -\min\}$ and $\{+\min, +\max\}$. The latter two configurations map to each other if the decay chains are defined as described above.

4. Example: SUSY higgs decaying to gauginos at the LHC

In order to demonstrate some of the simpler aspects of the above discussion a Monte Carlo study was conducted of heavy SUSY higgs particles decaying to the four lepton plus E_T^{miss} final state via $\tilde{\chi}_2^0 \tilde{\chi}_2^0$ with three-body $\tilde{\chi}_2^0$ lepton producing decays:

$$H/A \rightarrow \tilde{\chi}_2^0 \tilde{\chi}_2^0 \rightarrow \ell \ell \ell \ell \tilde{\chi}_1^0 \tilde{\chi}_1^0. \quad (4.1)$$

The model chosen for study was the mSUGRA *Point A* model from Ref. [9], for which $m(H/A) = 256$ GeV, $m(\tilde{\chi}_2^0) = 110$ GeV and $m(\tilde{\chi}_1^0) = 60$ GeV. The ISASUGRA 7.69 [21] RGE code coupled to HDECAY [22] was used to generate the sparticle mass spectra and branching ratios, while HERWIG 6.510 [23, 24] and ACERDET [25] were used to generate and simulate 14 TeV LHC events corresponding to about 300 fb^{-1} of data (assuming

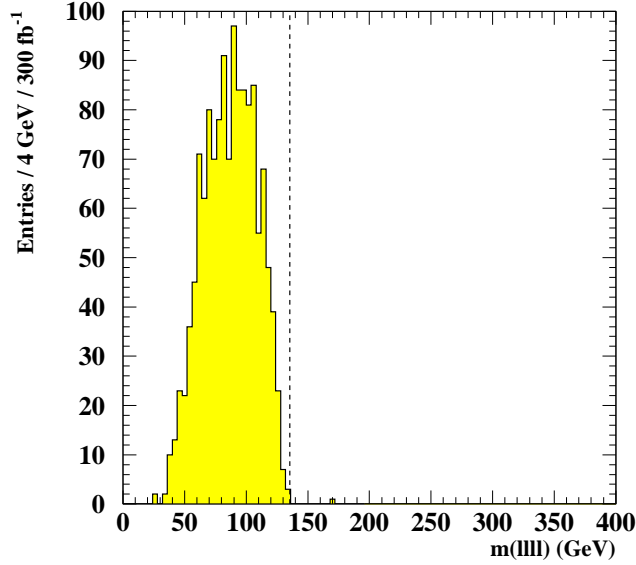


Figure 3: Distribution of detector-level four-lepton invariant mass values for $H/A \rightarrow \tilde{\chi}_2^0 \tilde{\chi}_2^0 \rightarrow \ell\ell\ell\ell\tilde{\chi}_1^0\tilde{\chi}_1^0$ events from the *Point A* model. The dashed vertical line represents the expected end-point position from Eqn. (2.2). The small population of events lying beyond the expected end-point is generated by detector mis-measurement.

perfect identification efficiency). Detailed studies of SM and SUSY backgrounds to the $4\ell + E_T^{\text{miss}}$ channel analysis are beyond the scope of this paper – for this simple illustrative study only signal events were considered with a rudimentary detector level event selection requiring merely the presence of four isolated leptons in opposite-sign same-flavour pairs. The resulting values of $m(v_1, v_2) = m(\ell_1, \ell_2, \ell_4, \ell_4)$, $M_T(0)$ and $M_T(2m(\tilde{\chi}_1^0))$ are shown in Figures 3 and 4.

In the case of $H/A \rightarrow \tilde{\chi}_2^0 \tilde{\chi}_2^0 \rightarrow \ell\ell\ell\ell\tilde{\chi}_1^0\tilde{\chi}_1^0$ events the two δ_i decay chains are identical, with $\omega \equiv H/A$, $\delta_1 = \delta_2 = \tilde{\chi}_2^0$, $\alpha_1 = \alpha_2 = \tilde{\chi}_1^0$ and $v_1 = v_2 = \ell^+\ell^-$. In the example considered here $m_{\text{max}}(v_i) = m(\tilde{\chi}_2^0) - m(\tilde{\chi}_1^0)$ due to the three-body nature of the $\tilde{\chi}_2^0$ decays, while $m_{\text{min}}(v_i) = 0$. Consequently the requirement in Eqn. (2.3) is satisfied and hence $m_{\text{max}}(v_1, v_2) = m(H/A) - 2m(\tilde{\chi}_1^0) = 136$ GeV. The requirement in Eqn. (3.7) is also satisfied giving $M_T^{\text{max}}(2m(\tilde{\chi}_1^0)) = 256$ GeV. The $M_T(0)$ end-point is given by Eqn. (3.6) leading to $M_T^{\text{max}}(0) = 180$ GeV. These expected end-point positions are represented in Figures 3 and 4 by vertical dashed lines and agree well with the observed end-points. It is interesting to note that the larger number of configurations saturating the bound on $M_T(2m(\tilde{\chi}_1^0))$ compared with $m(v_1, v_2)$ in this case leads to a more prominent end-point with a steeper gradient. This is true even at detector-level following smearing of the event E_T^{miss} values used to calculate $M_T(2m(\tilde{\chi}_1^0))$.

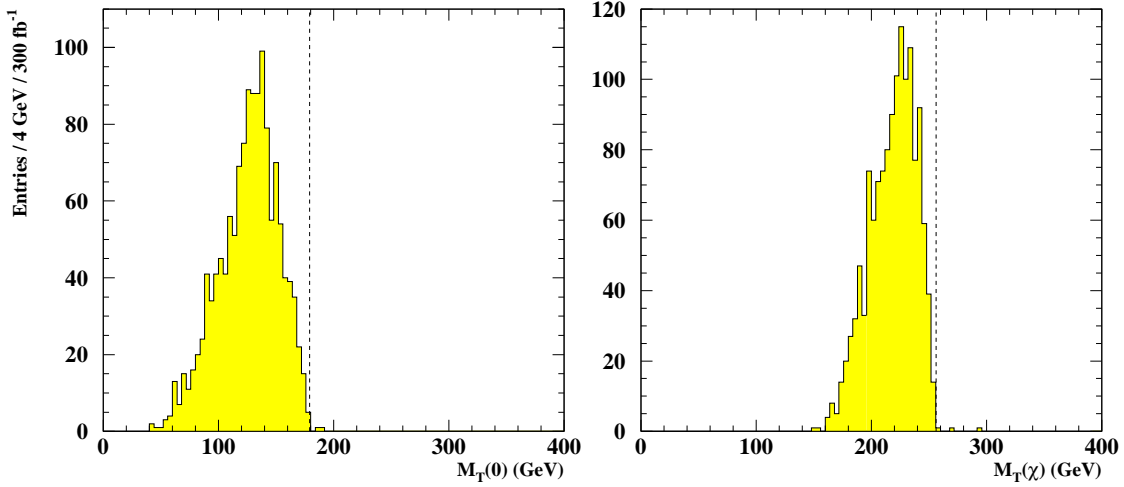


Figure 4: Distributions of detector-level transverse mass values for $H/A \rightarrow \tilde{\chi}_2^0 \tilde{\chi}_2^0 \rightarrow \ell\ell\ell\ell\tilde{\chi}_1^0 \tilde{\chi}_1^0$ events the *Point A* model. In the left(right)-hand figure the transverse mass is defined by Eqn. (3.1) (Eqn. (3.3)). The dashed vertical lines represent the expected end-point positions, given by respectively Eqn. (3.6) and $m(\omega)$. The small populations of events lying beyond the expected end-point are generated by detector mis-measurement.

5. Conclusions

This brief paper has discussed the positions of end-points in the invariant mass and transverse mass distributions of the decay products of heavy particles decaying to pairs of semi-invisibly decaying products. The formulae presented here may prove useful for mass measurements if SUSY higgs bosons decaying to gauginos are observed at the LHC. The same techniques may also prove useful in other new physics scenarios, for instance given heavy states decaying via pairs of new W' bosons to massive stable right-handed neutrinos.

Acknowledgements

DRT wishes to thank Alan Barr, Ben Gripaios, Chris Lester and Giacomo Polesello for helpful comments. DRT wishes to acknowledge STFC and the Leverhulme Trust for support.

References

- [1] H. Baer, M. Bisset, D. Dicus, C. Kao and X. Tata, Phys. Rev. D **47** (1993) 1062.
- [2] H. Baer, M. Bisset, C. Kao and X. Tata, Phys. Rev. D **50** (1994) 316 [arXiv:hep-ph/9402265].
- [3] M. A. Bisset, PhD Thesis, University of Hawaii (1995).

- [4] F. Moortgat, S. Abdullin and D. Denegri, arXiv:hep-ph/0112046.
- [5] M. Bisset, F. Moortgat and S. Moretti, Eur. Phys. J. C **30** (2003) 419 [arXiv:hep-ph/0303093].
- [6] M. M. Nojiri, G. Polesello and D. R. Tovey, arXiv:hep-ph/0312317.
- [7] C. Charlot, R. Salerno and Y. Sirois, J. Phys. G **34** (2007) N1.
- [8] G. Bian, M. Bisset, N. Kersting, Y. Liu and X. Wang, Eur. Phys. J. C **53** (2008) 429 [arXiv:hep-ph/0611316].
- [9] M. Bisset, J. Li, N. Kersting, F. Moortgat and S. Moretti, JHEP **0908** (2009) 037 [arXiv:0709.1029 [hep-ph]].
- [10] M. Bisset, J. Li and N. Kersting, arXiv:0709.1031 [hep-ph].
- [11] P. Huang, N. Kersting and H. H. Yang, Phys. Rev. D **77** (2008) 075011 [arXiv:0801.0041 [hep-ph]].
- [12] S. Gentile [ATLAS Collaboration], ATL-PHYS-PROC-2008-077;
- [13] S. Gentile [ATLAS Collaboration], ATL-PHYS-PROC-2009-020;
- [14] G. Arnison *et al.* [UA1 Collaboration], Phys. Lett. B **122** (1983) 103.
- [15] M. Banner *et al.* [UA2 Collaboration], Phys. Lett. B **122** (1983) 476.
- [16] G. Arnison *et al.* [UA1 Collaboration], Phys. Lett. B **129** (1983) 273.
- [17] B. Gripaios, JHEP **0802** (2008) 053 [arXiv:0709.2740 [hep-ph]].
- [18] A. J. Barr, B. Gripaios and C. G. Lester, JHEP **0802** (2008) 014 [arXiv:0711.4008 [hep-ph]].
- [19] A. J. Barr, B. Gripaios and C. G. Lester, JHEP **0907** (2009) 072 [arXiv:0902.4864 [hep-ph]].
- [20] A. J. Barr, B. Gripaios and C. G. Lester, JHEP **0911** (2009) 096 [arXiv:0908.3779 [hep-ph]].
- [21] F. E. Paige, S. D. Protopopescu, H. Baer and X. Tata, arXiv:hep-ph/0312045.
- [22] A. Djouadi, J. Kalinowski and M. Spira, Comput. Phys. Commun. **108** (1998) 56 [arXiv:hep-ph/9704448].
- [23] G. Corcella *et al.*, JHEP **0101** (2001) 010 [arXiv:hep-ph/0011363].
- [24] S. Moretti, K. Odagiri, P. Richardson, M. H. Seymour and B. R. Webber, JHEP **0204** (2002) 028 [arXiv:hep-ph/0204123].
- [25] E. Richter-Was, arXiv:hep-ph/0207355.